

# Study of the surface layer in cBN growth by PVD techniques

Q. Li<sup>a</sup>, S.F. Wong<sup>b,\*</sup>, W.M. Lau<sup>a</sup>, C.W. Ong<sup>b</sup>

<sup>a</sup> Department of Physics, The Chinese University of Hong Kong, Shatin, New Territory, Hong Kong, PRC

<sup>b</sup> Department of Applied Physics and Materials Research Center, The Hong Kong Polytechnic University, Hung Hom, Kowloon, Hong Kong, PRC

Received 18 April 2006; received in revised form 19 July 2006; accepted 22 August 2006

Available online 4 October 2006

## Abstract

A  $sp^2$  bonded boron nitride ( $sp^2$  BN) surface layer is sometimes observed on top of cubic boron nitride (cBN) grains for BN films deposited using ion-assisted PVD techniques. Understanding the formation of such surface layer gives a clue to the cBN growth mechanisms. In the current study, the microstructure and phase composition near the top surface of several BN films were investigated in order to clarify the formation mechanism of such a surface layer. All the films investigated were synthesized using ion-assisted PVD techniques, but with different deposition parameters. It was found that such a surface layer is not necessarily present in some of the cBN growth, and its presence depends on the bombardment of ion energy during deposition. The cBN growth mechanisms are discussed based on these observations.

© 2006 Elsevier B.V. All rights reserved.

**Keywords:** Cubic boron nitride; Ion-assisted PVD techniques;  $sp^2$  bonded boron nitride surface layer; Growth mechanisms

## 1. Introduction

It is generally understood that the growth of cubic boron nitride (cBN) films follows a layered sequence, i.e. an amorphous layer is first deposited on the substrate, followed by a layer of turbostratic BN (tBN), after which the cBN starts to nucleate and grow [1–3]. It has been noticed that in some samples, a fourth layer is present on top of the cubic phase, and is characterized to be  $sp^2$  bonded BN ( $sp^2$  BN) [3,4]. For the physical vapor deposition (PVD) process, where ion bombardment is usually incorporated to ensure cBN nucleation and growth, this observation becomes direct evidence supporting the subsurface growth mechanisms of the cubic phase [5]. It is also argued that the chemical vapor deposition of cBN may be ascribed to other mechanisms due to the absence of this specific surface layer. Nevertheless, the formation mechanism of the  $sp^2$  BN surface layer is not clear, which directly affects the interpretation of the cBN growth mechanism. Moreover, many TEM observations of the surface layer itself are susceptible. As most of the TEM sample preparation processes require ion milling at the last stage to achieve electron transparency, and Ar ions (with a voltage of  $\sim 4$  kV, typically used in ion-mill thinning) are

known to induce irradiation damage to the cubic phase, which could transform to  $sp^2$  BN. It is sometimes arguable whether the  $sp^2$  BN surface layer results from the deposition process or the TEM sample preparation process (in those cases where the epoxy glue is not present on the sample's top surface).

Surface layers in several cBN films deposited by different PVD methods including bias-assisted magnetron sputtering and dual-ion beam deposition (DIBD) [6,7] were studied. Using the latter method, a  $sp^2$  BN surface layer is observed in BN films deposited with a nitrogen ion energy of 450 eV, such a surface layer can be eliminated by post-deposition nitrogen ion bombardment at 100 eV. No surface layer is present in the case of magnetron sputtering, where the bombarding ion energy is  $\sim 100$  eV. These experimental observations suggest that thickening of the cBN layer is governed by certain subsurface growth mechanisms. The cBN growth is a dynamic process with ion penetration-grain growth, ion irradiation damage and sputter-etching operating at the same time.

## 2. Experimental methods

Sample A was deposited using rf-magnetron sputtering using a hexagonal BN target. The substrate temperature ( $T_s$ ) was maintained at 450 °C, and the substrate bias at  $-100$  V. The detailed deposition parameters can be found elsewhere [6].

\* Corresponding author. Fax: +852 2333 7629.

E-mail address: [96586087@alumni.polyu.edu.hk](mailto:96586087@alumni.polyu.edu.hk) (S.F. Wong).

Sample B1 was deposited by using DIBD at  $T_s=680$  °C. In this process, an argon ion ( $\text{Ar}^+$ ) beam was generated by one ion gun to sputter a 4-inch boron target. Meanwhile, the substrate was bombarded simultaneously by an assist  $\text{Ar}^+/\text{N}_2^+$  ion beam produced by another ion gun for the growth of the cBN layer, with the beam energy and current set at 450 eV and 30 mA respectively [7]. Sample B2 was deposited at exactly the same condition as Sample B1. The only difference is that N ions at 10 mA and 100 eV were introduced to bombard the film surface for 10 min after deposition. Silicon (100) wafers were used as the substrates for all the samples. The microstructure and the local chemical bonding information of the BN films were investigated using transmission electron microscopy (TEM). A JEOL 3000 FEG-TEM was used for TEM imaging. The electron energy loss spectroscopy (EELS) of the films was performed using a Gatan imaging filtering (GIF) system attached to the same microscope.

### 3. Results and discussion

A layered growth sequence is observed for all three samples. The film starts with a thin amorphous layer, followed by a layer of turbostratic BN (tBN). This layer can be either oriented tBN with its (0002) planes preferably parallel to the growth direction, or randomly oriented, depending on different deposition parameters. The BN phases in this layer can be identified to both hexagonal and rhombohedral, respectively (details will be discussed in separate publications), after which the cubic phase starts to nucleate and grow.

The top surface structures of these three samples appear to be different. Fig. 1 shows the microstructure of Sample A (magnetron sputtering, with  $-100$  V substrate bias) in the near surface region. The measured d-spacing of the fringes is 0.209 nm, matching with the theoretical value of cBN (111) d-spacing [8]. EEL spectrum taken from the same region also confirms the  $\text{sp}^3$  bonded BN ( $\text{sp}^3$  BN) content. The phase composition in the transition region across the  $\text{sp}^3$  BN and

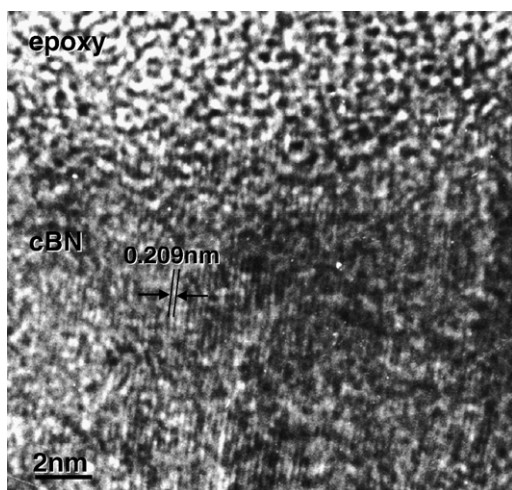


Fig. 1. High-resolution TEM image taken from Sample A, showing the structure of BN film close to the film top surface. Only the cBN phase is observed directly underneath the amorphous epoxy glue.

epoxy regions was carefully observed with EELS. Result shows that the characteristic features of the  $\text{sp}^3$  BN phase disrupt sharply across the boundary, indicating that there is no other phase, like the  $\text{sp}^2$  bonded BN ( $\text{sp}^2$  BN) phase, in-between.

As a comparison, high-resolution TEM image taken from the near surface region of Sample B1 is shown in Fig. 2(a). A surface layer of  $\sim 3$  nm is observed between the top of the cBN grain and the epoxy glue. The fringes in this layer appear to be randomly oriented with a relatively large spacing, distinguishing itself from the cubic phase and the epoxy layer. The spacing of these fringes is measured to be 0.366 nm, which agrees with the d-spacing of the tBN (0002) planes. The EEL spectrum [Fig. 2(b)] was taken from this surface layer by focusing the electron beam on it (EELS operated in the diffraction mode). The probe size of the electron beam is  $\sim 2$  nm. The two edges at 191 eV and 401 eV correspond to the energy loss (K-edge loss) characteristics of boron and nitrogen, respectively. The near-edge structure of the B K-edge spectra [Fig. 2(b)] consists of a sharp  $\pi^*$  peak, a broad  $\sigma^*$  peak, and an additional sharp peak [9]. The appearance of the  $\pi^*$  peak at 191 eV indicates that the surface layer consists of  $\text{sp}^2$  BN. It is interesting to note that the preferential orientation of the fringes appears in some part of the top layer. These  $\text{sp}^2$  BN lie with its (0002) planes parallel to the film surface.

When the surface of the as-deposited Sample B1 is sputter-cleaned by  $\sim 100$  eV nitrogen ions after deposition, this  $\text{sp}^2$  BN disappears. Fig. 3 shows a high-resolution TEM image taken from the near surface region in Sample B2. The microstructure is similar to that in Sample A, i.e., cBN is observed to be directly in contact with the epoxy glue, while no other layer exists in-between. This assertion was confirmed by investigating the EEL spectra across the  $\text{sp}^3$  BN and epoxy regions, where no sign of  $\text{sp}^2$  BN was observed.

Based on the above experimental results and literatures, we now address the cBN growth process, i.e., the expansion of cBN grains once nucleated. Generally speaking, ion bombardment contributes to the BN film growth in the following three aspects: (1) momentum transfer to the constitutional atoms (ions) through collision; (2) creating defects in the existing cBN grains; and (3) re-sputtering of the materials on the top surface. Process (1) makes it possible for the constitutional B and N ions to penetrate into the subsurface layer, and contribute to the cBN grain growth. Process (2) is the so-called ion irradiation damage. For ions penetrating into the subsurface layer, their energies decrease with the penetration depth. We note that the penetration range of a particle with 100–500 eV is about 1–2 nm according to the simulation by TRIM, which is fairly close to the dimension of the surface layer observed [10,11]. While the deeper-penetrated ions may contribute to the cBN grain growth, the shallow penetrated ions are expected to create a larger amount of defects than those can be repaired by the self-recovering process. The accumulation of these defects eventually leads to lattice damage and phase transformation from cBN to tBN. This argument was supported by the result of a recent study, which showed that argon ion irradiation with energy and fluency of 500 eV and  $5 \times 10^{16}$  ions  $\text{cm}^{-2}$  on a cBN crystal can drive a substantial portion of the cBN phase within the ion

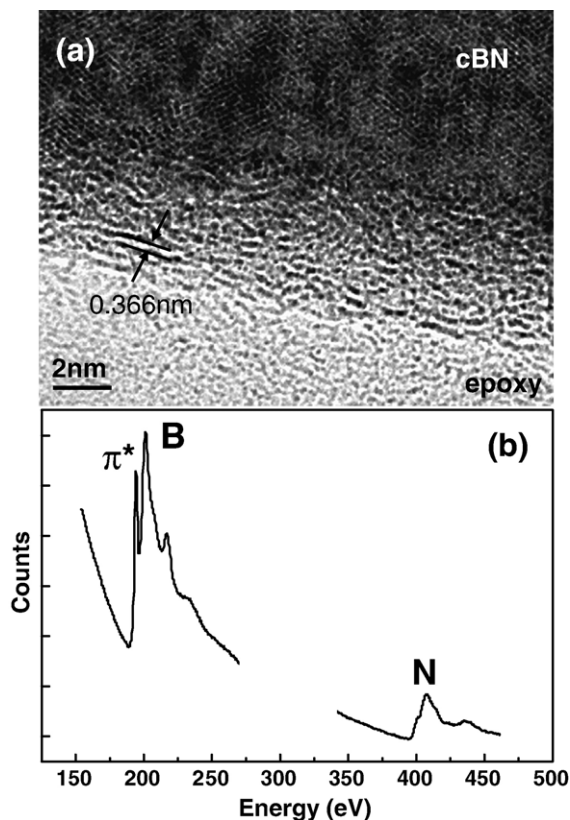


Fig. 2. (a) High-resolution TEM image taken from Sample B1. A non-cBN layer is observed at the film's top surface, covering the cBN grains underneath. (b) Electron energy loss spectroscopy (EELS) taken from the surface layer shown in (a), with electron beam focused to  $\sim 1$  nm size. The EEL spectrum suggests that the surface layer is composed of  $sp^2$  BN.

penetration depth of 1.1 nm to transform into the hexagonal BN and amorphous BN phases [12]. Process (3) is mainly an etching process. Obviously the sputter yield depends on both the nature of the materials and the bombarding ion energy [11].

Therefore, the cBN growth is a dynamic process with the above mechanisms operating simultaneously. The existence of

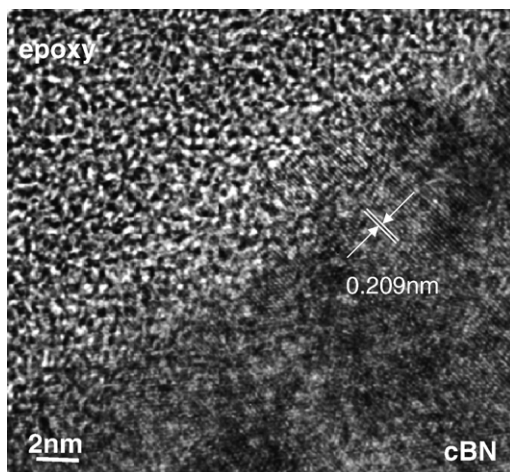


Fig. 3. High-resolution TEM image taken from Sample B2, showing the structure of the BN film close to the film top surface. Only cBN is observed.

ion energy threshold for cBN growth [13], the  $sp^2$  BN surface layer observed in samples deposited with high ion energy [14], and the theoretical TRIM calculation [11] supports the sub-surface growth model for cBN. The absence of the  $sp^2$  BN surface layer in Sample A does not contradict with such model. At low ion energies (above the cBN growth threshold, but relatively low), little cubic phase would be irradiation damaged (transform to  $sp^2$  BN) at the top surface region, and it will be easily sputter-etched if formed ( $sp^2$  BN have a higher sputter yield than  $sp^3$  BN [15]). In fact, this is consistent with our previous study of ion irradiation damage of cBN single crystal using Ar ions [12]. Little phase transformation ( $<5\%$  cBN to tBN) is induced by the ion bombardment when the ion energy is less than 200 eV. Theoretical simulation indicates that at this ion energy range, the B and N atoms in the cBN lattice may be displaced by the penetrating ions (defects formation), considering that the knock-on displacement energy of a B or N atom is in the order of a few tens of eV [13]. However, they immediately undergo a self-recovery process and retain the cubic lattice. This argument is further strengthened by the difference observed in Samples B1 and B2. The 100 eV nitrogen ions only sputter-clean the film surface region without further introducing any  $sp^2$  BN on top of cBN. As the tBN surface layer is highly defected, and thus a loose structure, it is easy to be sputtered off by low energy ion bombardment.

It is also indicated by a previous study [12] that severe irradiation damage will be caused ( $>82\%$  cBN transformed into tBN considering ion penetration depth of 1.1 nm), when the ion energy is increased above 500 eV. Again, this is consistent with the presented experimental data of Sample B1 (deposited using 450 eV nitrogen ion).

Although the current experimental setting does not allow us to explore even higher ion energy regions, we may speculate that a similar effect can be observed. In fact, Hofsäss et al. have observed a  $sp^2$  BN surface layer covering the cBN grains underneath in a film deposited using 5 keV ion beam [14]. The existence of such surface layer results from the equilibrium between the ion irradiation damage (layer creating) and sputter-etching (layer eliminating). Intuitively, controlled conditions have to be achieved, so that the  $sp^2$  BN surface layer can be within a certain thickness, which allows the deep-penetrated B and N species to reach the cubic phase and contribute to further growth.

We refer to some other published data in literature [14,16–18], and find that the arguments proposed in this study are further supported. As summarized in Fig. 4, for cBN films deposited with low energy species, such as chemical vapor deposition (CVD) with negative bias voltages below  $-40$  V

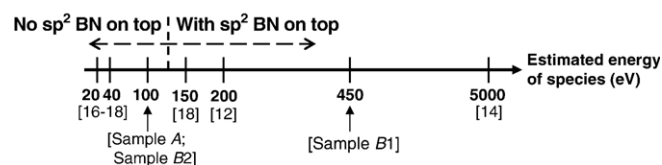


Fig. 4. A schematic summary showing how the energy of the species involved in a deposition process influences the appearance of  $sp^2$  BN phase on the top surface of cBN film.



[16–18], the films do not have  $sp^2$  BN on top. This is consistent with the result of Samples A and B2, which involved the use of 100 eV species in deposition such that ion-induced  $sp^3$ -to- $sp^2$  transition was not significant and any  $sp^2$  residue on the film surface would be sputtered clean readily. With the use of species with higher energies, such as CVD process with negative bias voltages beyond  $-100$  eV [18], ion-induced  $sp^3$ -to- $sp^2$  transition becomes more severe. Hence, like Sample B1, the  $sp^2$  BN phase was formed and left on the film surface.

We finally point out an interesting fact that orientation of (0002) planes in the surface  $sp^2$  BN layer varies among different cases. The (0002) planes appear to be either relatively randomly oriented or approximately parallel to the film surface in the current study, but are parallel to the film growth direction in the work of Hofsäss et al. [14]. Intuitively, the surface tBN with its (0002) planes parallel to the film surface will minimize the dangling bonds, and thus have the lowest surface energy. However, this is not consistent with the experimental observations. Whether such orientation will affect the cBN growth process is not clear.

#### 4. Conclusions

cBN growth is a dynamic process with ion penetration-grain growth, ion irradiation damage and sputter-etching operating simultaneously. At high ion energy levels, a  $sp^2$  BN surface layer can be continuously created due to the ion irradiation damage, which is explained by the shallow ion penetration induced defects accumulation. cBN can be grown at low energy ion bombardment ( $<100$  eV) [19–21], in which range little irradiation damage occurs. Although the ions at this energy level are capable of displacing the B and N atoms in the cBN lattice, such displacement can be repaired by the self-recovering process. On the other hand, these ions can sputter the loose tBN phase without much affecting the cubic phase. Therefore, the absence of  $sp^2$  BN surface layer does not necessarily indicate a non-subsurface growth mechanism.

#### Acknowledgements

The authors are indebted to the assistance of Prof. Cockayne in Oxford University regarding the TEM work. The work

described in this paper was substantially supported by a grant from the Research Grants Council of the Hong Kong Administrative Region (Project No.: PolyU 5141/00E, account code: B-Q362) and an internal grant from the Hong Kong Polytechnic University.

#### References

- [1] A. Klett, R. Freudenstein, W. Kulisch, M. Ye, M.P. Delplancke-Ogletree, *Thin Solid Films* 398 (2001) 279.
- [2] H. Feldermann, C. Ronning, H. Hofsäss, Y.L. Huang, M. Seibt, *J. Appl. Phys.* 90 (2001) 3248.
- [3] P.B. Mirkarimi, K.F. McCarty, D.L. Medlin, *Mater. Sci. Eng., R Rep.* 21 (1997) 47.
- [4] K.F. McCarty, D.L. Medlin, *Diamond Relat. Mater.* 6 (1997) 1219.
- [5] Y. Lifshitz, S.R. Kasi, J.W. Rabalais, *Phys. Rev. Lett.* 62 (1987) 1290.
- [6] Q. Li, I. Bello, L.D. Marks, Y. Lifshitz, S.T. Lee, *Appl. Phys. Lett.* 80 (2002) 46.
- [7] S.F. Wong, C.W. Ong, G.K.H. Pang, Q. Li, W.M. Lau, *Diamond Relat. Mater.* 13 (2004) 1632.
- [8] W.L. Zhou, Y. Ikuhara, T. Suzuki, *Appl. Phys. Lett.* 67 (1995) 3551.
- [9] D.R. McKenzie, W.D. McFall, W.G. Sainty, C.A. Davis, R.E. Collins, *Diamond Relat. Mater.* 2 (1993) 970.
- [10] H. Hofsäss, H. Feldermann, R. Merk, M. Sebastian, C. Ronning, *Appl. Phys., A* 66 (1998) 153.
- [11] Y. Lifshitz, S.R. Kasi, J.W. Rabalais, *Phys. Rev., B* 41 (1990) 10468.
- [12] Y.Y. Hui, K.W. Wong, W.M. Lau, *J. Vac. Sci. Technol., A, Vac. Surf. Films* 20 (2002) 1774.
- [13] P.B. Mirkarimi, K.F. McCarty, D.L. Medlin, W.G. Wolfer, T.A. Friedmann, E.J. Klaus, G.F. Cardinale, D.F. Howitt, *J. Mater. Res.* 9 (1994) 2925.
- [14] H. Hofsäss, H. Feldermann, S. Eyhusen, C. Ronning, *Phys. Rev., B* 65 (2002) 115410.
- [15] S. Reinke, M. Kuhr, W. Kulisch, *Diamond Relat. Mater.* 3 (1994) 341.
- [16] H.S. Yang, C. Iwamoto, T. Yoshida, *J. Appl. Phys.* 95 (2004) 2337.
- [17] W.J. Zhang, C.Y. Chan, X.M. Meng, M.K. Fung, I. Bello, Y. Lifshitz, S.T. Lee, X. Jiang, *Angew. Chem., Int. Ed. Engl.* 44 (2005) 4749.
- [18] X.M. Meng, W.J. Zhang, C.Y. Chan, C.S. Lee, I. Bello, S.T. Lee, *Appl. Phys. Lett.* 88 (2006) 031904.
- [19] J. Hahn, F. Richter, R. Pintaske, M. Röder, E. Schneider, T. Welzel, *Surf. Coat. Technol.* 92 (1997) 129.
- [20] J. Ye, H. Oechsner, S. Westermeyr, *J. Vac. Sci. Technol., A, Vac. Surf. Films* 19 (2001) 2294.
- [21] D. Litvinov, R. Clarke, *Appl. Phys. Lett.* 71 (1997) 1969.